

Supporting Information

A Flower-Inspired Divergent Light-Trapping Structure with Quasi-Spherical Symmetry towards a High-Performance Flexible Photodetector

Sixiang Liu,^a Junlong Tian,^{a,*} Shu Wu,^a Xilin Jia,^a Minyuan Luo^a and Wang Zhang^b

^a Hunan Key Laboratory of Micro-Nano Energy Materials and Devices, Laboratory for Quantum Engineering and Micro-Nano Energy Technology, School of Physics and Optoelectronic, Xiangtan University, Hunan 411105, P. R. China.

^b State Key Laboratory of Metal Matrix Composites, Shanghai Jiao Tong University, 800 Dongchuan Road, Shanghai 200240, P. R. China.

*Author to whom correspondence should be addressed: jltian666@xtu.edu.cn

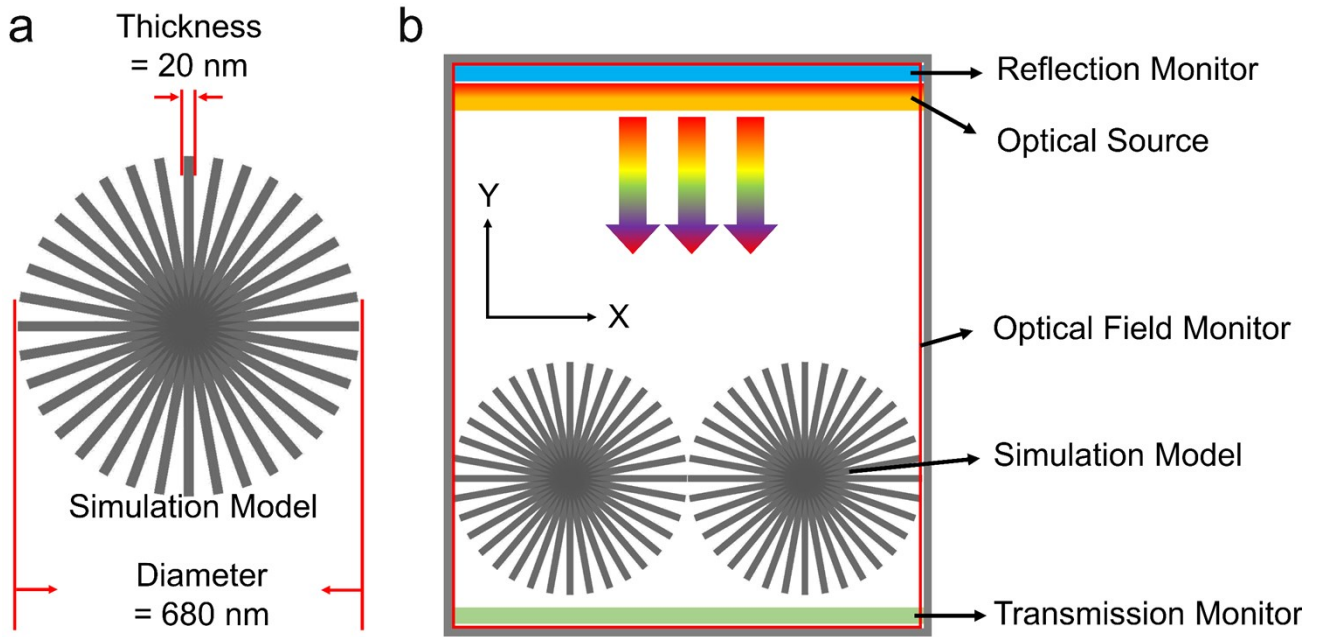


Figure S1. (a) Schematic diagrams of MoS₂_F. (b) Schematic illustrations of the FDTD simulations of MoS₂_F.

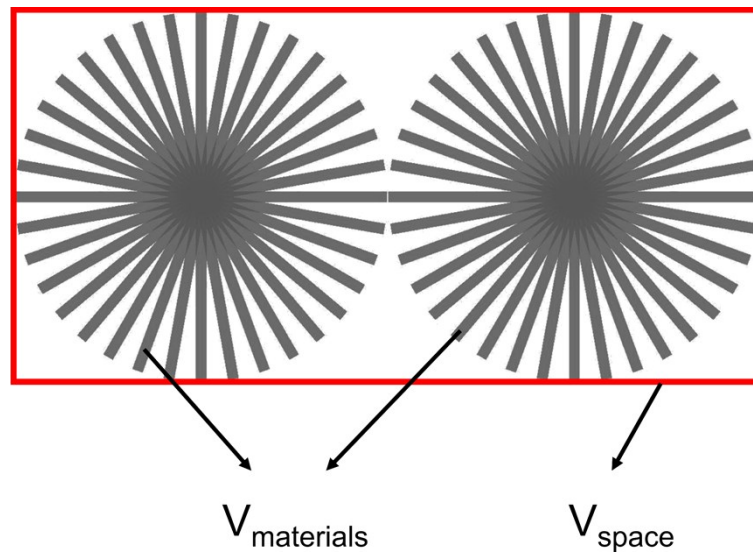


Figure S2. Schematic diagrams of volume of materials and volume of the space where the material is located.

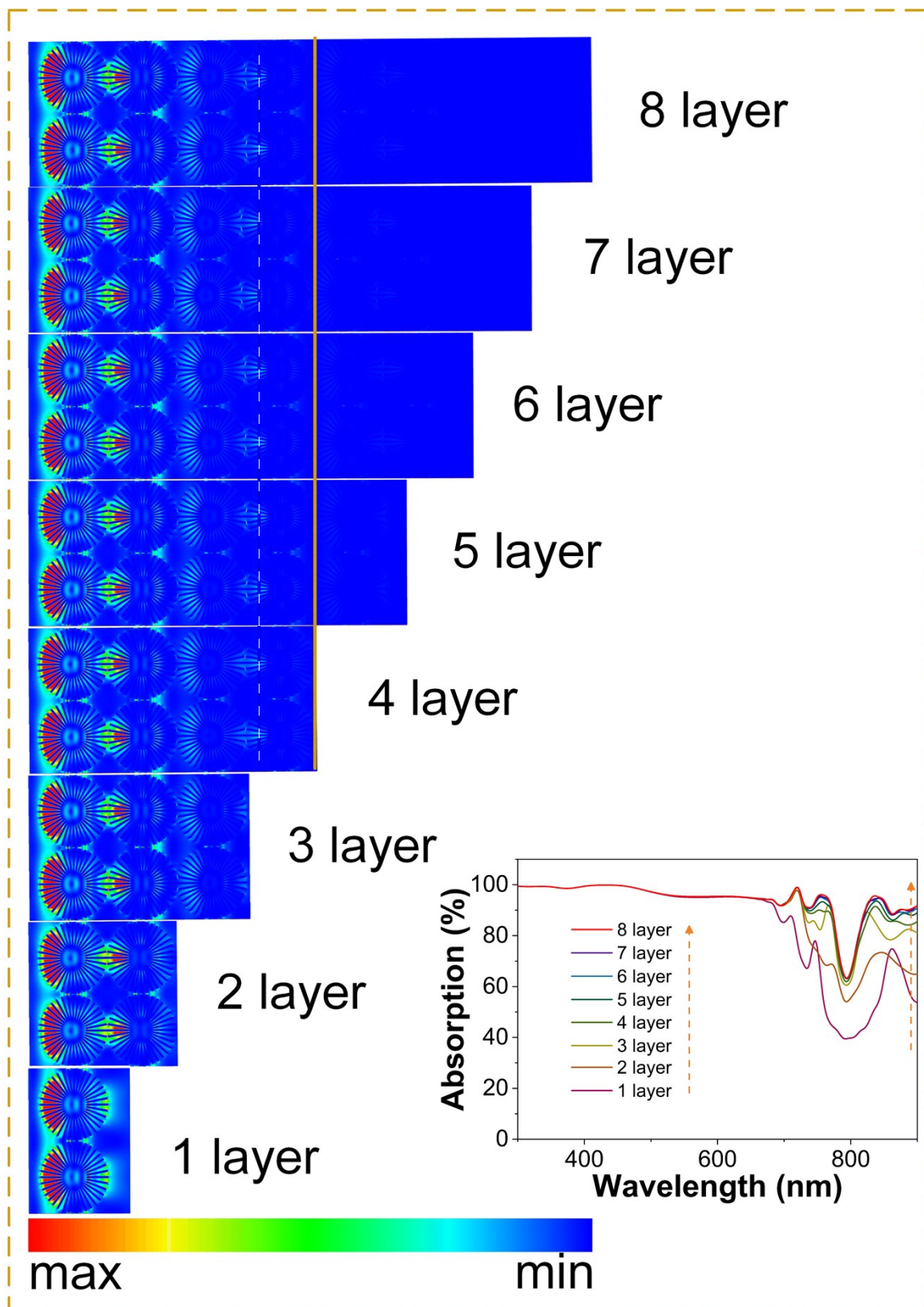


Figure S3. The electric field distribution ($|E|^2$) of 1 to 8 layers of $\text{MoS}_2\text{-F}$, respectively. The insert is the light absorption of 1 to 8 layers of $\text{MoS}_2\text{-F}$.

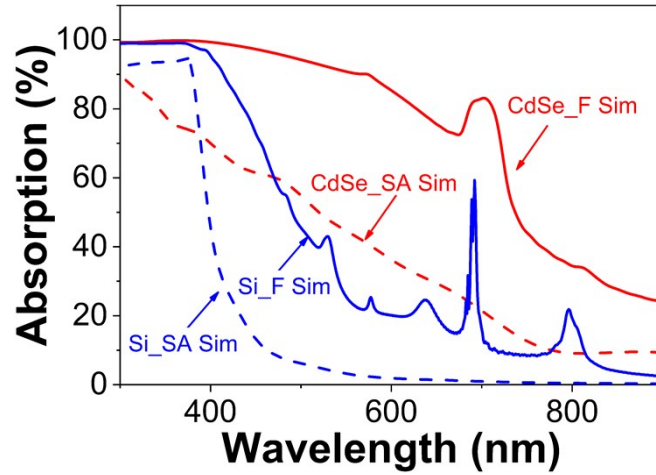


Figure S4. FDTD simulation of Light absorption of Si_SA, Si_F, CdSe_SA, and CdSe_F under the same D_{ratio} of 43.9% with the wavelength range of 300-900 nm, respectively.

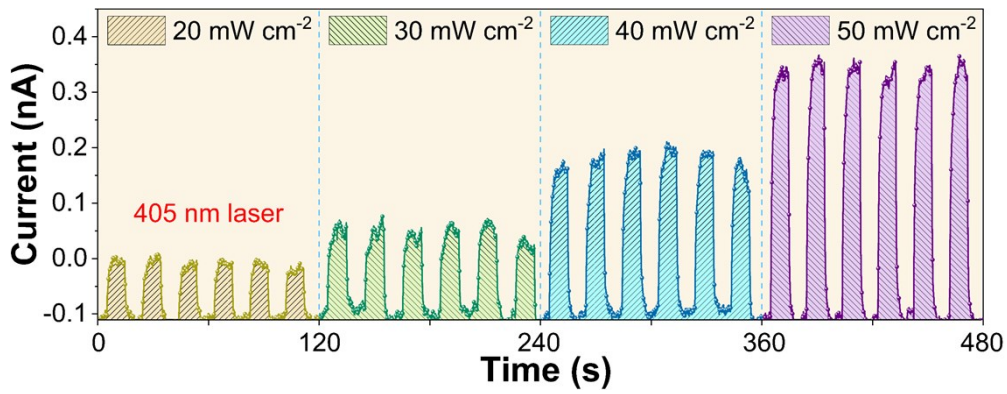


Figure S5. $I-t$ characteristics of the self-powered PD under 405 nm laser illumination with different power densities from 20 to 50 mW cm^{-2} at zero bias.

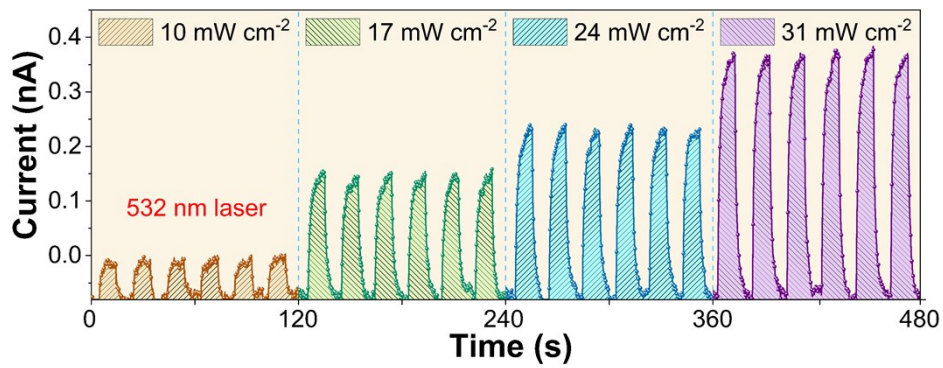


Figure S6. $I-t$ characteristics of the self-powered PD under 532 nm laser illumination with different power densities from 10 to 31 mW cm^{-2} at zero bias.

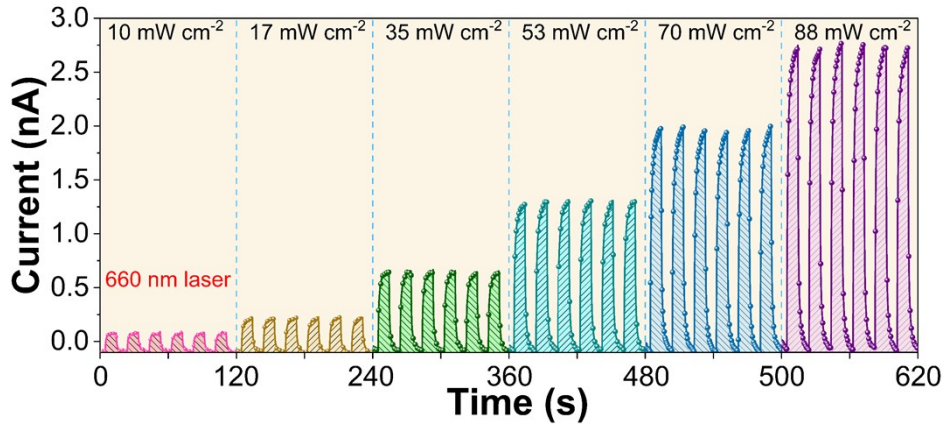


Figure S7. *I-t* characteristics of the self-powered PD under 660 nm laser illumination with different power densities from 10 to 88 mW cm⁻² at zero bias.

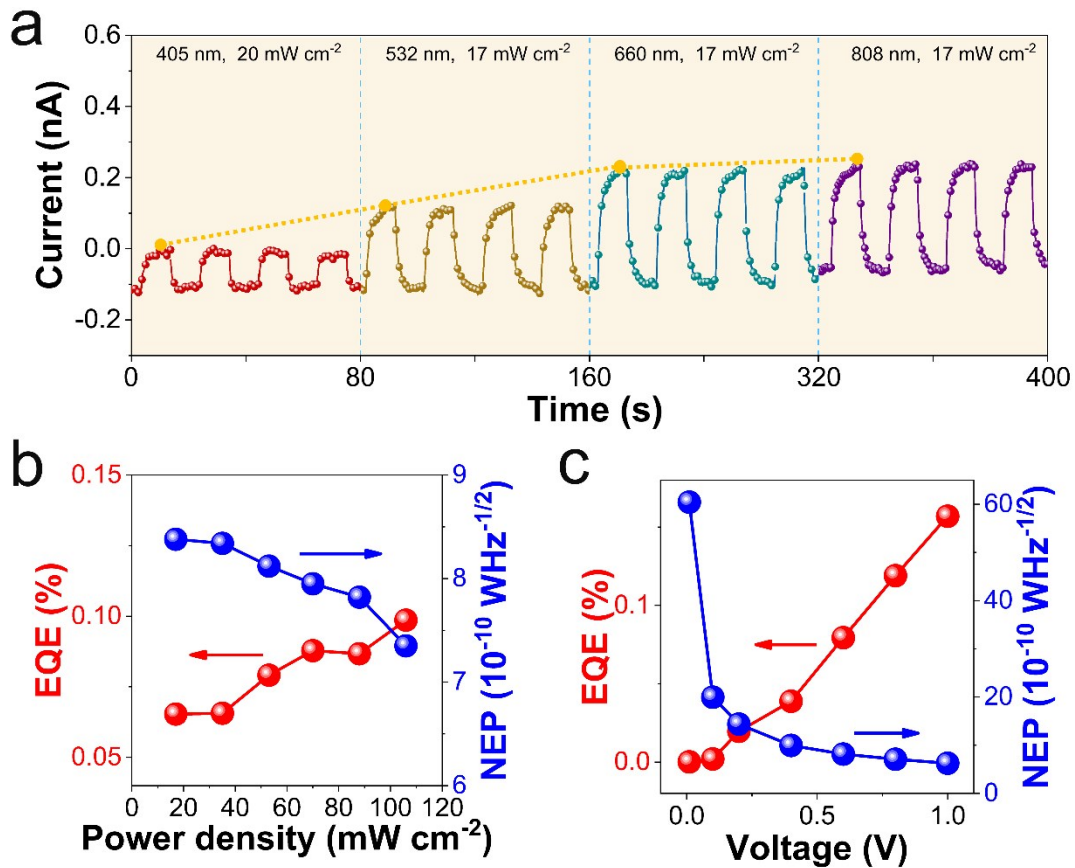


Figure S8. (a) Photoresponse behaviors of the self-powered PD under 405, 532, 660, and 808 nm laser illuminations at 0 V bias voltage. (b) The external quantum efficiency (EQE) and noise equivalent power (NEP) of the PD as a function of power density under 808 nm laser at zero bias. (c) The external quantum efficiency (EQE) and noise equivalent power (NEP) of the PD as a function of voltage under 808 nm laser with a power density of 106 mW cm⁻².

External quantum efficiency (EQE)^{1,2} and noise equivalent power (NEP)¹⁻³ can be calculated by the following equation:

$$EQE = R \times [hc/(e\lambda)],$$

$$NEP = \sqrt{2eI_d/R}$$

$$\text{or } NEP = (R \times \sqrt{A_0})/D,$$

where R is the responsibility at λ wavelength, h is Planck's constant, c is the speed of light, e is the elementary charge, λ is the incident light wavelength, I_d is the dark current, A_0 is the active area of the fabricated device, and D is the detectivity of the PD. As is shown in **Figure S8c**, the EQE and NEP of the fabricated device can reach to 0.2% and $6.27 \times 10^{-10} \text{ WHz}^{-1/2}$ at 1 V. Contrary to detectivity, the lower the NEP value, the better. The result shows that the increase in voltage can enhance the performance of PD to a certain extent, because the applied bias can promote the movement of carriers and then enhance the PD's performance. **Figure S8b** shows that the increase in power density is benefit to the PD's performance at zero bias.

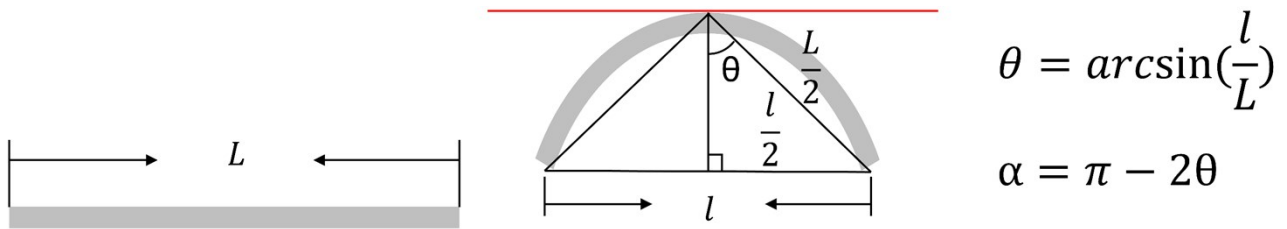


Figure S9. Schematic diagram of device bending and calculation formula of bending angle α .

Table S1. The bending angle α corresponding to the bending stages of the flexible device.

Bending states	I	II	III	IV	I
α	0°	58°	103°	151°	0°

Table S2. Performance comparison of MoS₂-based photonic devices.

Materials	Wavelength (nm)	Bias (V)	Responsibility (mA/W)	Detectivity (Jones)	Reference
pristine MoS ₂ nanosheets	980	0	2×10^{-4}	120 ± 80	Yu et al. ⁴
rhodamine 6G-treated MoS ₂ nanosheet	980	0	6×10^{-4}	300 ± 200	Yu et al. ⁴
single-layer MoS ₂ nanosheet	550	0	0.42	-	Yin et al. ⁵
MoTe ₂ /MoS ₂ nanosheet	1550	0.8	17×10^{-3}	-	Zhang et al. ⁶
MoS ₂ with Au nano-antenna arrays	830	0	0.013	-	Hou et al. ⁷
MoS ₂ nanosheet arrays	532	0	6	-	Rahmati et al. ⁸
MoS ₂ _F	808	1	1.4	3.4×10^5	This work
MoS ₂ _F	808	0	6.5×10^{-3}	2.7×10^5	This work

References

1. M. Buscema, J. O. Island, D. J. Groenendijk, S. I. Blanter, G. A. Steele, H. S. J. van der Zant and A. Castellanos-Gomez, *Chem. Soc. Rev.*, 2015, **44**, 3691-3718.
2. R. K. Ulaganathan, Y.-Y. Lu, C.-J. Kuo, S. R. Tamalampudi, R. Sankar, K. M. Boopathi, A. Anand, K. Yadav, R. J. Mathew, C.-R. Liu, F. C. Chou and Y.-T. Chen, *Nanoscale*, 2016, **8**, 2284-2292.
3. L. Goswami, N. Aggarwal, M. Singh, R. Verma, P. Vashishtha, S. K. Jain, J. Tawale, R. Pandey and G. Gupta, *ACS Appl. Nano Mater.*, 2020, **3**, 8104-8116.
4. S. H. Yu, Y. Lee, S. K. Jang, J. Kang, J. Jeon, C. Lee, J. Y. Lee, H. Kim, E. Hwang, S. Lee and J. H. Cho, *ACS Nano*, 2014, **8**, 8285-8291.
5. Z. Yin, H. Li, H. Li, L. Jiang, Y. Shi, Y. Sun, G. Lu, Q. Zhang, X. Chen and H. Zhang, *ACS Nano*, 2012, **6**, 74-80.
6. K. Zhang, T. Zhang, G. Cheng, T. Li, S. Wang, W. Wei, X. Zhou, W. Yu, Y. Sun, P. Wang, D. Zhang, C. Zeng, X. Wang, W. Hu, H. J. Fan, G. Shen, X. Chen, X. Duan, K. Chang and N. Dai, *ACS Nano*, 2016, **10**, 3852-3858.
7. C. Hou, Y. Wang, L. Yang, B. Li, Z. Cao, Q. Zhang, Y. Wang, Z. Yang and L. Dong, *Nano Energy*, 2018, **53**, 734-744.
8. B. Rahmati, I. Hajzadeh, R. Karimzadeh and S. M. Mohseni, *Appl. Surf. Sci.*, 2018, **455**, 876-882.